



ISSN 2278 – 0211 (Online)

## Heat Transfer of Nanofluid Past an Exponentially Permeable Stretching Sheet with Heat Generation and Newtonian Heating in a Porous Medium

**M. Lavanya**

Research Scholar, Department of Applied Mathematics, Y. V. University, Kadapa, Andhra Pradesh, India

**Dr. M. Sreedhar Babu**

Assistant Professor, Department of Applied Mathematics, Y. V. University, Kadapa, Andhra Pradesh, India

**G. Venkata Ramanaiah**

Research Scholar, Department of Applied Mathematics, Y. V. University, Kadapa, Andhra Pradesh, India

### **Abstract:**

*In present study, we have investigated the phenomenon of Newtonian heating under the application of uniform porous medium when heat generation and chemical reaction appears in the energy and volumetric species equations in the flow of a nanofluid. The flow is induced by an exponentially permeable stretching sheet. The solutions of the nonlinear equations governing the velocity, temperature and nanoparticle volume fraction profiles are solved numerically using Runge-Kutta Gill procedure together with shooting method and graphical results for the resulting parameters are displayed and discussed. The influence of the physical parameters on skin-friction coefficient, local Nusselt number and nanoparticle Sherwood number are shown in a tabulated form.*

**Keywords:** porous medium, nanoparticle, Newtonian heating, heat generation and chemical reaction.

### **1. Introduction**

Nanofluids are the fluid suspensions of nanoparticles showing many interesting properties and distinctive features. Al, Cu, Fe and Titanium or their oxides are the most frequently used nanoparticles. The similar physical and chemical properties are consisted by the materials with the sizes of nanometers. This led to the study of nanofluids in a variety of processes which resulted in notable applications in engineering and sciences. On account of its practical applications in industries, a great deal of attention is being paid to the research works on convective heat transfer in nanofluids in porous medium. Choi (1995) introduced the term nanofluids to refer to the fluid with suspended nanoparticles. Choi et al (2001) confirmed that the addition of a small amount of nanoparticles to conventional heat transfer liquids increases the thermal conductivity of the fluid up to approximately two times. Buongiorno (2006) discussed convective transport in nanofluids. He reported that only Brownian diffusion and thermophoresis are essential slip mechanisms in nanofluids.

The flow phenomena in porous media have its applications in a wide range of disciplines covering chemical engineering to geophysics. Both heat and mass transfer phenomenon in porous media is recently emphasized because of its applications. Wang and Tu (1989), Anand Rao et al. (2015) revealed the effect of porous medium in boundary layer problems. It shows the decrease in velocity profile and the increase in temperature profile. Mandal and Mukhopadhyay (2013) observed the heat transfer analysis for fluid flow over an exponentially stretching porous sheet with surface heat flux in porous medium.

In many realistic cases, the heat transfer from the surface is proportional to the local surface temperature. Such an effect is known as Newtonian heating effect. Merkin (1994) studied conjugate convective flow with Newtonian heating. Due to various applications researchers are attracted to consider the Newtonian heating condition in their problems. Hussanan et al. (2013) obtained an exact analysis of mass and heat transfer past a vertical plate with Newtonian heating. Recently, the unsteady boundary layer flow and heat transfer of a Casson fluid under the Newtonian heating boundary condition for non-Newtonian fluid was investigated by Hussanan et al. (2014). Das et al. (2015) carried out the work on Newtonian heating on unsteady heat and mass transfer of Casson flow over a vertical plate by taking the effects of thermal radiation. Ram Reddy et al. (2015) investigated the free convection flow on a permeable vertical plate of a micropolar fluid under the convective boundary condition is obtained using Lie group transformations and concluded that a raise in Biot number  $Bi$  decreases concentration distribution, whereas it causes an enhanced in temperature distribution, skin friction and wall couple stress coefficients, and heat and mass transfer rates.

In present study, we have studied the phenomenon of Newtonian heating under the application of uniform porous medium when heat generation and chemical reaction appears in the energy and volumetric species equations in the flow of a nanofluid. The flow is induced by an exponentially permeable stretching sheet. The solutions of the nonlinear equations governing the velocity, temperature and nanoparticle volume fraction profiles are solved numerically using Runge-Kutta Gill procedure together with shooting technique and graphical results for the resulting parameters are displayed and discussed. The influence of physical parameters on skin-friction coefficient, local Nusselt number and nanoparticle Sherwood number are shown in a tabulated form.

## 2. Mathematical Formulation

Consider the steady boundary layer flow of heated nanofluid over an exponentially stretching sheet in a porous medium. With the usual Boussinesq and the boundary layer approximations, the governing equations of continuity, momentum, energy and Volumetric species are written as follows [Battacharyya and Layek (2014), Khan and Pop (2010)];

$$\frac{\partial u'}{\partial x} + \frac{\partial v'}{\partial y} = 0 \quad (2.1)$$

$$u' \frac{\partial u'}{\partial x} + v' \frac{\partial u'}{\partial y} = v \frac{\partial^2 u'}{\partial y^2} - \frac{v}{k(x)} u' \quad (2.2)$$

$$u' \frac{\partial T}{\partial x} + v' \frac{\partial T}{\partial y} = \alpha \frac{\partial^2 T}{\partial y^2} + \frac{(\rho c)_p}{(\rho c)_f} \left[ D_B \frac{\partial N}{\partial y} \frac{\partial T}{\partial y} + \frac{D_T}{T_\infty} \left( \frac{\partial T}{\partial y} \right)^2 \right] + \frac{q(x)}{(\rho c_p)_f} (T - T_\infty) \quad (2.3)$$

$$u' \frac{\partial N}{\partial x} + v' \frac{\partial N}{\partial y} = D_B \frac{\partial^2 N}{\partial y^2} + \frac{D_T}{T_\infty} \frac{\partial^2 T}{\partial y^2} - k'(x) (N - N_\infty) \quad (2.4)$$

The suitable boundary conditions are

$$u' = U_w, v' = 0, \frac{\partial T}{\partial y} = -h_1 T, \frac{\partial N}{\partial y} = -h_1 N \quad \text{at } y = 0$$

$$u' \rightarrow 0, T \rightarrow T_\infty, N \rightarrow N_\infty \quad \text{as } y \rightarrow \infty \quad (2.5)$$

Where  $u'$  &  $v'$  are the velocity components in  $x$  - direction &  $y$ - direction, respectively,  $\nu$  be kinematic viscosity and  $\alpha$  be thermal conductivity,  $k(x) = 2k_0 e^{x/2L}$  be non-uniform permeability of the medium,  $k_0$  be constant which give the initial permeability,  $q(x) = q_0 e^{x/L}$  be heat source coefficient,  $k'(x) = 2k_1 e^{x/L}$  be initial chemical reaction coefficient,  $h_1$  be heat transfer coefficient,  $h_2$  be mass transfer coefficient,  $\rho_f$  be density of the base fluid,  $(\rho c)_f$  and  $(\rho c)_p$  are heat capacities of base fluid and nanoparticles, respectively,  $T$  be the temperature,  $D_B$  be Brownian diffusion coefficient,  $N$  be nanoparticle volumetric fraction,  $D_T$  be thermophoretic diffusion coefficient and  $T_\infty$  be temperature of the fluid outside the boundary layer,  $T_w$  be variable temperature at the sheet with  $T_0$  being a constant which measures the rate of temperature increase along the sheet,  $N_w$  be variable wall nanoparticle volume fraction with  $N_0$  being a constant, and  $N_\infty$  be constant nanoparticle volume fraction in free stream.

The stretching velocity  $U_w$  is given by

$$U_w(x) = c e^{\frac{x}{L}} \quad (2.6)$$

where  $c > 0$  is stretching constant.

The equation of continuity is satisfied for the choice of a stream function

$\psi(x, y)$  such that

$$u' = \psi_y \quad \text{and} \quad v' = \psi_x \quad (2.7)$$

where  $\psi(x, y)$  is the stream function.

In order to transform the equations (2.2) to (2.5) into a set of ordinary differential equations, the following similarity transformations and dimensionless variables are introduced.

$$\begin{aligned} \psi &= \sqrt{2\nu Lc} f(\eta) e^{\frac{x}{2L}}, \eta = y \sqrt{\frac{c}{2\nu L}} e^{\frac{x}{2L}} \\ \theta(\eta) &= \frac{T - T_\infty}{T_w - T_\infty}, \phi(\eta) = \frac{N - N_\infty}{N_w - N_\infty}, K = \frac{k_0 c}{\nu L} \\ Pr &= \frac{\nu}{\alpha}, Le = \frac{\nu}{D_B}, \delta = \frac{2Lq_0}{(\rho c_p)c} \\ Nb &= \frac{D_B (\rho c)_p (N_w - N_\infty)}{\nu (\rho c)_f}, Nt = \frac{D_T (\rho c)_p (T_w - T_\infty)}{T_\infty (\rho c)_f \nu} \\ \gamma &= h_1 \sqrt{\frac{2\nu L}{c}} e^{\frac{-x}{2L}}, \beta = h_2 \sqrt{\frac{2\nu L}{c}} e^{\frac{-x}{2L}}, Kr = \frac{k_1 L}{c} \end{aligned} \quad (2.8)$$

where  $f(\eta)$  be dimensionless stream function,  $\theta$  be dimensionless temperature,  $\phi$  be dimensionless nanoparticle volume fraction,  $\eta$  be similarity variable,  $K$  be local permeability parameter,  $\delta$  be the local heat generation parameter,  $Le$  be local Lewis number,  $Nb$  be local Brownian motion parameter,  $Nt$  be local thermophoresis parameter,  $Pr$  be local Prandtl number,  $Kr$  be local chemical reaction parameter,  $\gamma$  be local conjugate parameter for Newtonian heating,  $\beta$  be local conjugate parameter for concentration.

After the substitution of these transformations (2.8) along with the equation (2.7) into the Equations (2.2)-(2.6), the resulting non-linear ordinary differential equations are written as

$$f''' + ff'' - 2f'^2 - \frac{1}{K} f' = 0 \quad (2.9)$$

$$\theta'' + Pr(f\theta' - f'\theta) + Nb\theta'\phi' + Nt\theta'^2 + \delta\theta = 0 \quad (2.10)$$

$$\phi'' + Le(f\phi' - f'\phi) + \frac{Nt}{Nb}\theta'' - Kr\phi = 0 \quad (2.11)$$

together with the boundary conditions

$$\begin{aligned} f = 0, f' = 1, \theta' = -\gamma(1 + \theta), \phi' = -\beta(1 + \phi) \text{ at } \eta = 0 \\ f' \rightarrow 0, \theta \rightarrow 0, \beta \rightarrow 0 \text{ as } \eta \rightarrow \infty \end{aligned} \quad (2.12)$$

Physical quantities of interest are Local skin friction coefficient  $C_f$ , the heat transfer rate and mass transfer rate are the main physical characteristics of the problem, which are described in terms of local Nusselt number and local Sherwood number, respectively, defined as Hady et al. (2012).

$$C_f = \frac{\nu}{U_w^2 e^{2x/L}} \left( \frac{\partial u}{\partial y} \right)_{y=0}, Nu = \frac{-x}{(T_w - T_\infty)} \left( \frac{\partial T}{\partial y} \right)_{y=0}, Sh = \frac{-x}{(N_w - N_\infty)} \left( \frac{\partial N}{\partial y} \right)_{y=0} \quad (2.13)$$

or by introducing the transformations (2.9), we have

$$\sqrt{2Re_x} C_f = f''(0), \frac{Nu}{\sqrt{2Re_x}} = -\sqrt{\frac{x}{2L}} \theta'(0), \frac{Sh}{\sqrt{Re_x}} = -\sqrt{\frac{x}{2L}} \phi'(0) \quad (2.14)$$

Where  $Re_x = \frac{U_w x}{\nu}$  is the local Reynolds number.

### 3. Solution of the Problem

For solving equations (2.9)-(2.11), a step by step integration method i.e. Runge-Kutta method has been applied. For carrying in the numerical integration, the equations are reduced to a set of first order differential equation. For performing this we make the following substitutions:

$$\begin{aligned} y_1 = f, \quad y_2 = f', \quad y_3 = f'', \quad y_4 = \theta, \quad y_5 = \theta', \quad y_6 = \phi, \quad y_7 = \phi' \\ y_3' &= 2y_2^2 - y_1 y_3 + \frac{1}{K} y_2 \\ y_5' &= Pr(y_2 y_4 - y_1 y_5) - Nb y_5 y_7 - Nt y_5^2 - \delta y_4 \\ y_7' &= -Le(y_1 y_7 - y_2 y_6) - \frac{Nt}{Nb} (Pr(y_2 y_4 - y_1 y_5) - Nb y_5 y_7 - Nt y_5^2 - \delta y_4) + Kr y_6 \end{aligned} \quad (3.1)$$

The boundary conditions are given by (2.12) taking the form

$$\begin{aligned}
 y_1(0) &= 0, y_2(0) = 1, y_3(0) = -\gamma (1 + y_4(0)), y_7(0) = -\beta (1 + y_6(0)) \\
 y_2(\infty) &\rightarrow 0, y_4(\infty) \rightarrow 0, y_6(\infty) \rightarrow 0
 \end{aligned}
 \tag{3.2}$$

In order to carry out the step by step integration of equations (2.9)–(2.11), Gills procedures as given in Ralston and Wilf (1960) have been used. To start the integration, it is necessary to provide all the values of  $y_1, y_2, y_3, y_4, y_5, y_6$  at  $\eta = 0$  from which point, the forward integration has been carried out but from the boundary conditions it is seen that the values of  $y_3, y_4, y_7$  are not known. So we are to provide such values of  $y_3, y_4, y_7$  along with the known values of the other function at  $\eta = 0$  as would satisfy the boundary conditions as  $\eta \rightarrow \infty$  to a prescribed accuracy after step by step integrations are performed. Since the values of  $y_3, y_4, y_7$  which are supplied are merely rough values, some corrections have to be made in these values in order that the boundary conditions to  $\eta \rightarrow \infty$  are satisfied. These corrections in the values of  $y_3, y_4, y_7$  are taken care of by a self-iterative procedure which can for convenience be called ‘‘Corrective procedure’’.

#### 4. Results and Discussion

In order to acquire physical understanding, the velocity, temperature & nanoparticle volume fraction distributions have been illustrated by varying the numerical values of the various parameters demonstrated in the present problem. The numerical results are tabulated and exhibited with the graphical illustration.

The effect of permeability of the porous medium parameter (K) on the dimensionless velocity, temperature & nanoparticle volume fraction profiles for the fluid considered are shown in figures 1(a)-1(c). The other parameters are fixed as  $Pr = 2, Le = 2, Nt = 0.1, Nb = 0.1, \delta = 0.3, \gamma = 0.3, \beta = 0.3$  and  $Kr = 0.6$ . It is noticed that, with the hype in the values of K from 0.4 to 1.8 then the velocity increases consequently increases the momentum boundary layer region but the temperature and nanoparticle volume fraction of the fluid diminishes. The reason for this is, the permeability of the porous medium obstructs the fluid to move freely through the boundary layer. This leads to the raise in the thermal and concentration boundary layer region.

The effect of conjugate parameter for Newtonian heating ( $\gamma$ ) on the dimensionless temperature and & nanoparticle volume fraction profiles for the fluid considered are shown in figures 2(a) & 2(b). The other parameters are fixed as  $Pr = 2, K = 0.4, Le = 2, Nt = 0.1, Nb = 0.1, \delta = 0.3, \beta = 0.3$  and  $Kr = 0.6$ . It is observed that raising the values of  $\gamma$  from 0.1 to 0.4 the resultant temperature and nanoparticle volume fraction of the fluid increases consequently the thickness of thermal and concentration boundary layer enhances.

The effect of conjugate parameter for concentration ( $\beta$ ) on the dimensionless temperature & nanoparticle volume fraction profiles for the fluid considered are shown in figures 3(a) & 3(b). The other parameters are fixed as  $Pr = 2, Le = 2, Nt = 0.1, Nb = 0.1, \delta = 0.3, \gamma = 0.3, K = 0.4$  and  $Kr = 0.6$ . It is observed that raising the values of  $\beta$  from 0.1 to 1.2, the temperature and nanoparticle volume fraction of the fluid increases. This leads to enhance the thermal and nanoparticle concentration boundary layer region.

The effect of thermophoresis parameter (Nt) on the dimensionless temperature & nanoparticle volume fraction profiles for the fluid considered are shown in figures 4(a) & 4(b). The other parameters are fixed as  $Pr = 2, Le = 2, K = 0.4, Nb = 0.1, \delta = 0.3, \gamma = 0.3, \beta = 0.3$  and  $Kr = 0.6$ . It is conformed that enhances the values of Nt from 0.1 to 0.7, the temperature and nanoparticle volume traction of the fluid increases. This leads to increases the thermal and nanoparticle concentration boundary layer region.

The effect of Brownian motion parameter (Nb) on the dimensionless temperature & nanoparticle volume fraction profiles for the fluid considered are shown in figures 5(a) & 5(b). The other parameters are fixed as  $Pr = 2, Le = 2, K = 0.4, Nt = 0.1, \delta = 0.3, \gamma = 0.3, \beta = 0.3$  and  $Kr = 0.6$ . It is conformed that enhances the values of Nb from 0.1 to 1.0, the temperature increases but nanoparticle volume traction of the fluid decreases. In the system nanofluid, the Brownian motion takes a place in the presence of nanoparticles. When hype the values of Nb, the Brownian motion is affected and the nanoparticle concentration boundary layer thickness reduces and accordingly the heat transfer characteristics of the fluid changes.

The effect of Prandtl number (Pr) on the dimensionless temperature & nanoparticle volume fraction profiles for the fluid considered are shown in figures 6(a) & 6(b). The other parameters are fixed as  $Le = 2, K = 0.4, Nb = 0.1, Nt = 0.1, \delta = 0.3, \gamma = 0.3, \beta = 0.3$  and  $Kr = 0.6$ . it can be noticed that the dimensionless temperature and nanoparticle volume fraction are decreased on increasing Prandtl number. Physically, increasing Prandtl number becomes a key factor to reduce the thickness of the thermal and nanoparticle concentration boundary layers..

The effect of heat generation parameter ( $\delta$ ) on the dimensionless temperature profiles for the fluid considered are shown in figure 7. The other parameters are fixed as  $Pr = 2, Le = 2, K = 0.4, Nb = 0.1, Nt = 0.1, \delta = 0.3, \gamma = 0.3, \beta = 0.3$  and  $Kr = 0.6$ . It is observed that the thermal boundary layer thickness increases with raising the values of  $\delta$  from 0 to 0.3.

The effect of Lewis number (Le) on the dimensionless nanoparticle volume fraction profiles for the fluid considered is shown in figure 8. The other parameters are fixed as  $Pr = 2, \delta = 0.3, K = 0.4, Nb = 0.1, Nt = 0.1, \delta = 0.3, \gamma = 0.3, \beta = 0.3$  and  $Kr = 0.6$ . It is confirmed that the nanoparticle concentration distribution is significantly decreased while the values of Lewis number increased from 2 to 7.

The effect of chemical reaction parameter (Kr) on the dimensionless nanoparticle volume fraction profiles for the fluid considered is shown in figure 9. The other parameters are fixed as  $Pr = 2, \delta = 0.3, K = 0.4, Nb = 0.1, Nt = 0.1, \delta = 0.3, \gamma = 0.3, \beta = 0.3$  and  $Le = 2$ . It is confirmed that the nanoparticle concentration distribution is significantly decreased while the values of Kr increased from 0.1 to 1.5.

In order to standardize the method used in the present study and to decide the accuracy of the present analysis and to compare with the results available (Magyari and Keller (1999) and Bhattacharyya and Layek (2014)) relating to the local skin-friction coefficient in the absence of porous medium and found in an agreement (Table.1). Table 2 reveals the magnitude of skin fraction on different values of  $K$ . It is noticed that with the raise in values of  $K$  from 0.1 to 0.4, the resultant values of then  $|f''(0)|$  increases. Table 3 reveals the local Nusselt number and nanofluid Sherwood number on different parameters. It is noticed that with the raise in values of  $K$  from 0.1 to 0.4, the resultant values of then  $-\theta'(0)$  and  $-\phi'(0)$  decreases. With the raise in the values of  $Pr$  from 2 to 5, the resultant values of then  $-\theta'(0)$  decreases whereas  $-\phi'(0)$  increases. With the raise in the values of  $Nt$  from 0.1 to 0.6, the resultant values of  $-\theta'(0)$  and  $-\phi'(0)$  increases. With the raise in values of  $Nb$  from 0.1 to 0.6, the resultant values of  $-\theta'(0)$  increases whereas  $-\phi'(0)$  decreases. With the raise in the values of  $Le$  from 2 to 5, the resultant values of  $-\theta'(0)$  and  $-\phi'(0)$  is to be decreases. With the raise in the values of  $\delta$  from 0.1 to 0.3, the resultant values of  $-\theta'(0)$  and  $-\phi'(0)$  is to be increases. With the raise in the values of  $Kr$  from 0.1 to 1, the resultant values of  $-\theta'(0)$  and  $-\phi'(0)$  is to be increases. With the raise in the values of  $\gamma$  from 0.1 to 0.4, the resultant values of  $-\theta'(0)$  and  $-\phi'(0)$  is to be increases. Finally, with the raise in the values of  $\beta$  from 0.1 to 1, the resultant values of  $-\theta'(0)$  and  $-\phi'(0)$  is to be increases.

## 5. Conclusions

In this present paper numerically examined the nanofluid due to an exponentially permeable stretching sheet in the presence of porous medium, chemical reaction, heat generation and Newtonian heating. The important findings of the paper are:

- With the influence of permeability of the porous medium parameter, the fluid velocity increases, whereas temperature and nanoparticle volume fraction decreases.
- In the presence of thermophoresis parameter, the fluid temperature and mass volume fraction increases.
- In the vicinity of Brownian motion parameter, there is a hype in the fluid temperature and reduction in mass volume fraction.
- With the impact of heat generation, the fluid temperature enhances.
- With the effect of conjugate parameter for Newtonian heating and conjugate parameter for concentration, the fluid temperature and mass volume fraction increases.
- With the influence of permeability parameter, both the local Nusselt number and Shearwood number increases whereas the skin friction coefficient decreases.
- With the influence of heat generation parameter and chemical reaction parameter, the local Nusselt number and Sherwood number falls but the opposite results are found due to conjugate parameter for Newtonian heating and conjugate parameter for concentration.
- 

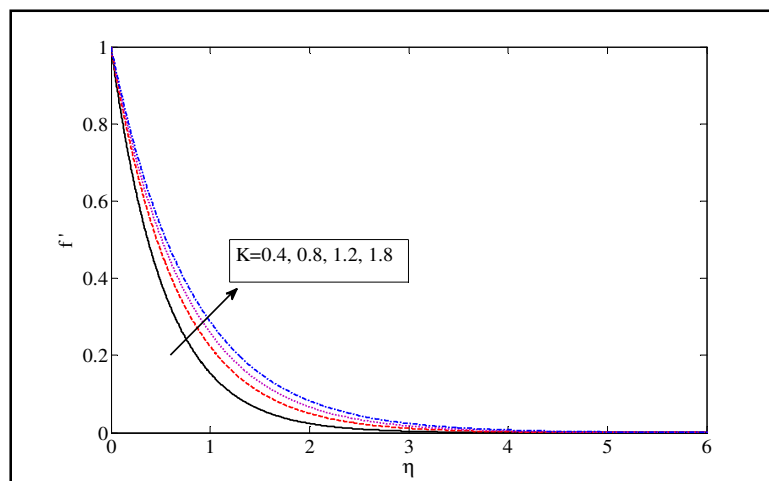


Figure 1(a): Velocity profiles for various  $K$  values for  $Pr = 2$ ,  $\gamma = 0.3$ ,  $Le = 2$ ,  $Nt = 0.1$ ,  $Nb = 0.1$ ,  $\delta = 0.3$ ,  $\beta = 0.3$  and  $Kr = 0.6$ .

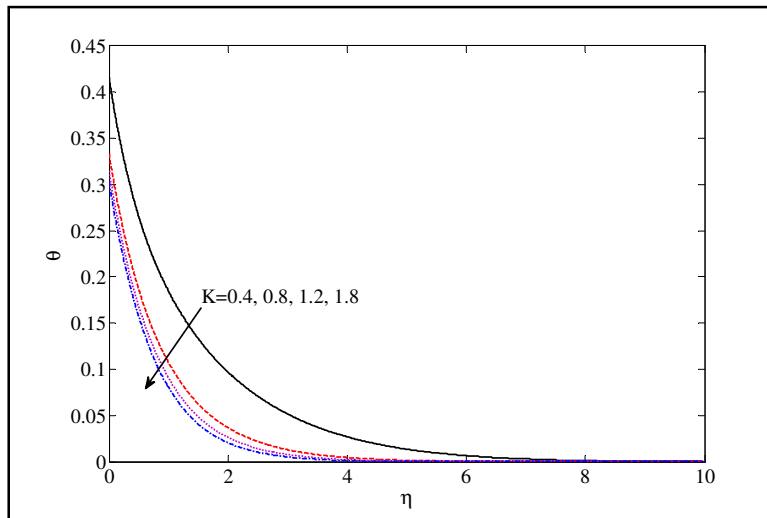


Figure 1(b): Temperature profiles for various  $K$  values for  $Pr = 2, \gamma = 0.3, Le = 2, Nt = 0.1, Nb = 0.1, \delta = 0.3, \beta = 0.3$  and  $Kr = 0.6$

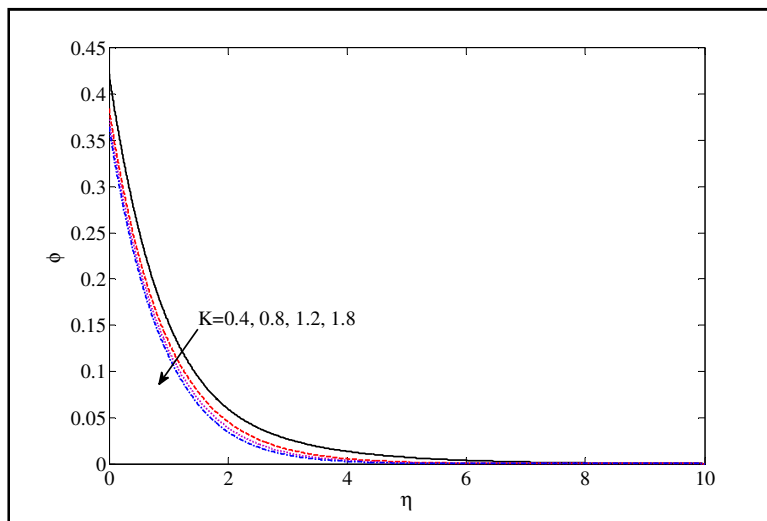


Figure 1(c): Nanoparticle volume fraction profile for various  $K$  values for  $Pr = 2, \gamma = 0.3, Le = 2, Nt = 0.1, Nb = 0.1, \delta = 0.3, \beta = 0.3$  and  $Kr = 0.6$

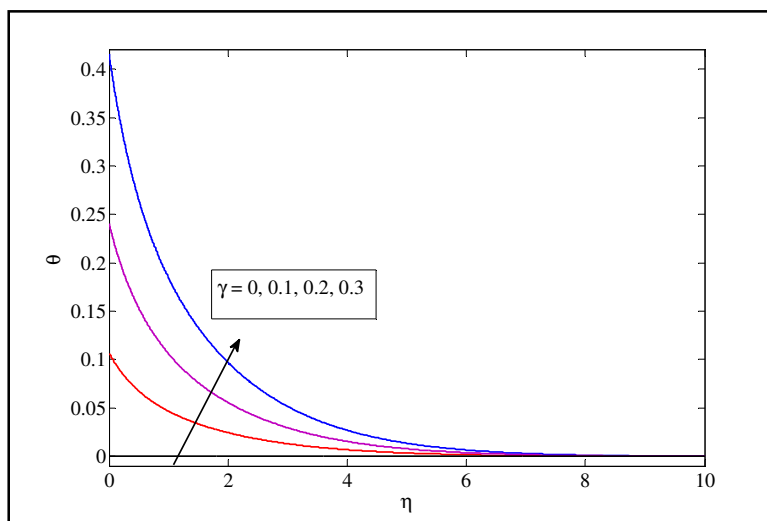


Figure 2(a): Temperature profile for various  $\gamma$  values for  $Pr = 2, K = 0.4, Le = 2, Nt = 0.1, Nb = 0.1, \delta = 0.3, \beta = 0.3$  and  $Kr = 0.6$

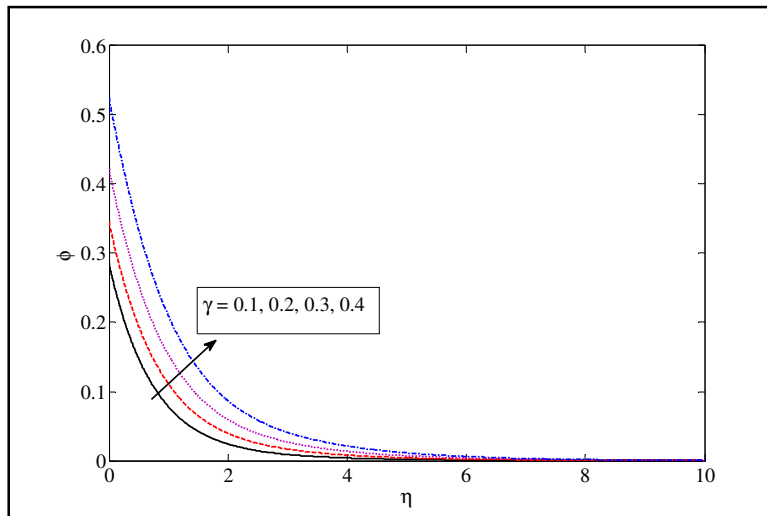


Figure 2(b): Nanoparticle volume fraction profile for various  $\gamma$  values for  $Pr = 2, K = 0.4, Le = 2, Nt = 0.1, Nb = 0.1, \delta = 0.3, \beta = 0.3$  and  $Kr = 0.6$

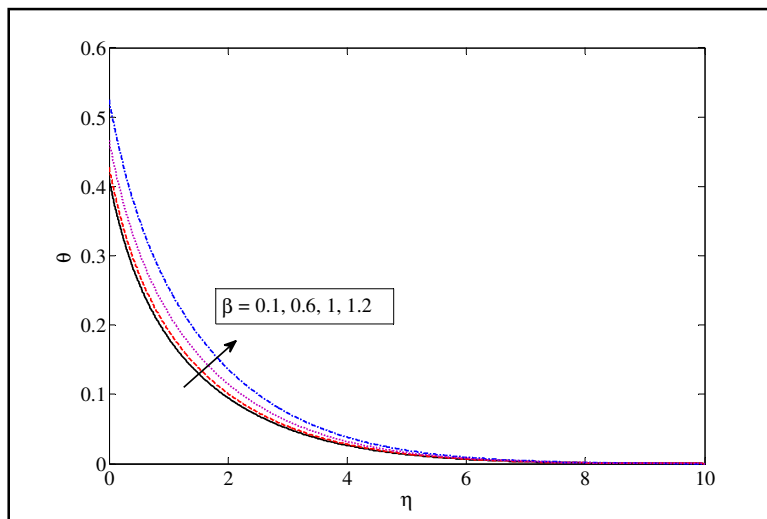


Figure 3(a): Temperature profile for various  $\beta$  values when  $Pr = 2, K = 0.4, Le = 2, Nt = 0.1, Nb = 0.1, \delta = 0.3, \gamma = 0.3$  and  $Kr = 0.6$

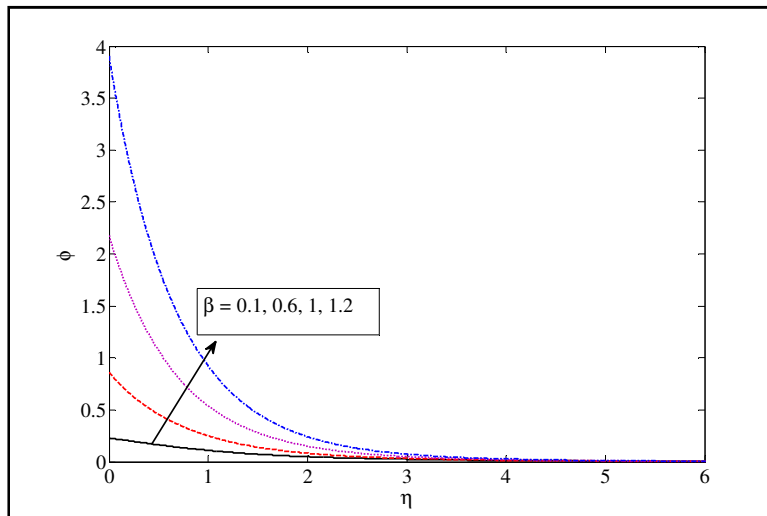


Figure 3(b): Nanoparticle volume fraction profile for various  $\beta$  values with  $Pr = 2, K = 0.4, Le = 2, Nt = 0.1, Nb = 0.1, \delta = 0.3, \gamma = 0.3$  and  $Kr = 0.6$

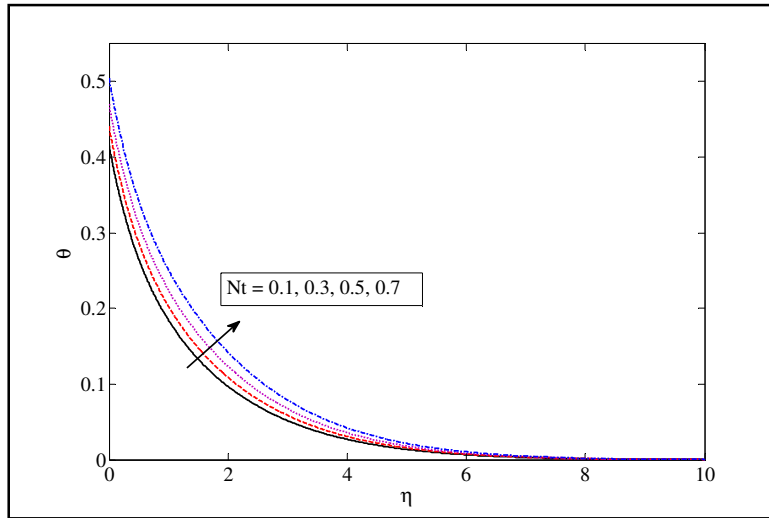


Figure 4(a): Temperature profile for various  $Nt$  values with  $Pr = 2, K = 0.4, Le = 2, \gamma = 0.3, Nb = 0.1, \delta = 0.3, \beta = 0.3$  and  $Kr = 0.6$

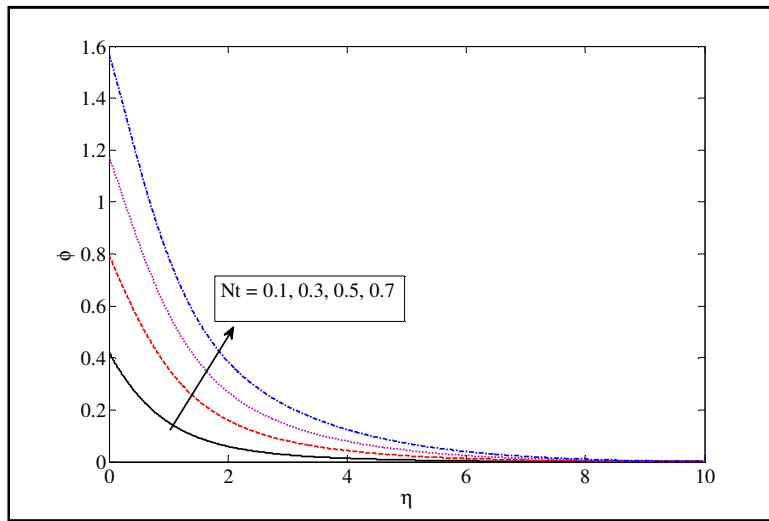


Figure 4(b): Nanoparticle volume fraction profile for various  $Nt$  values with  $Pr = 2, K = 0.4, Le = 2, \gamma = 0.3, Nb = 0.1, \delta = 0.3, \beta = 0.3$  and  $Kr = 0.6$

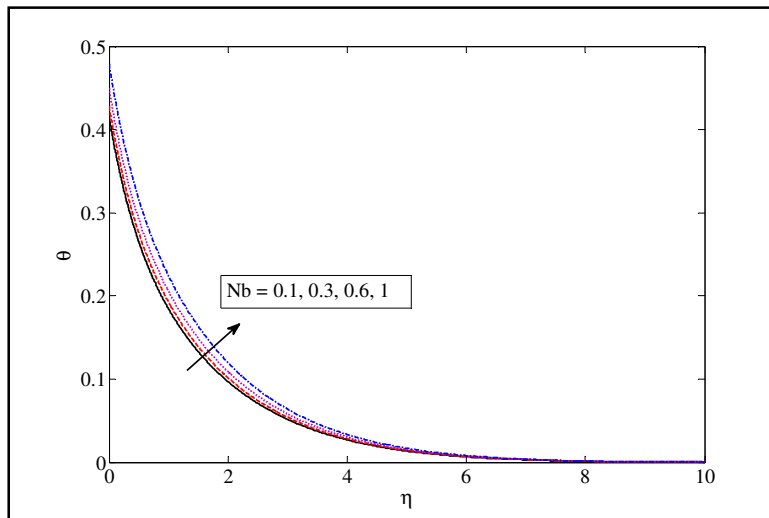


Figure 5(a): Temperature profile for various  $Nb$  values with  $Pr = 2, K = 0.4, Le = 2, Nt = 0.1, \gamma = 0.3, \delta = 0.3, \beta = 0.3$  and  $Kr = 0.6$

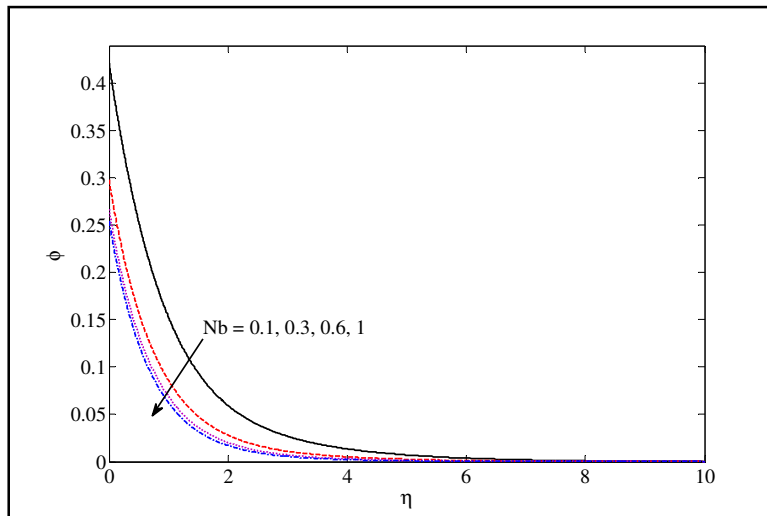


Figure 5(b): Nanoparticle volume fraction profile for various  $Nb$  values with  $Pr = 2, K = 0.4, Le = 2, Nt = 0.1, \gamma = 0.3, \delta = 0.3, \beta = 0.3$  and  $Kr = 0.6$

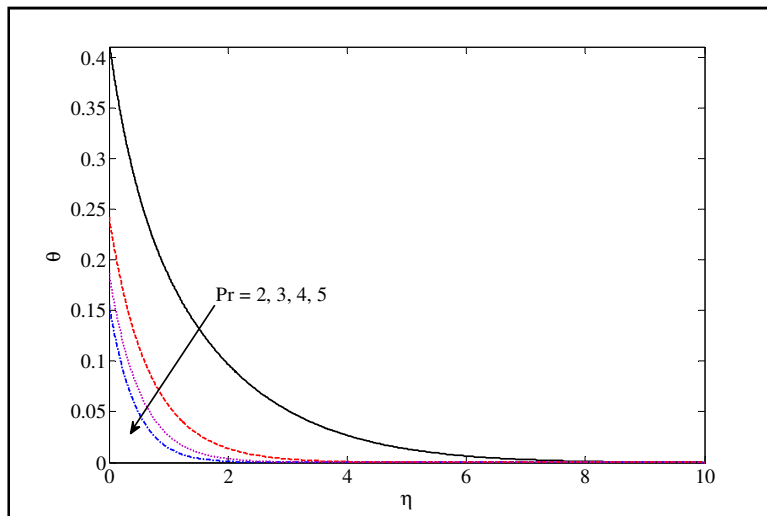


Figure 6(a): Temperature profile for various  $Pr$  values with  $\gamma = 0.3, K = 0.4, Le = 2, Nt = 0.1, Nb = 0.1, \delta = 0.3, \beta = 0.3$  and  $Kr = 0.6$

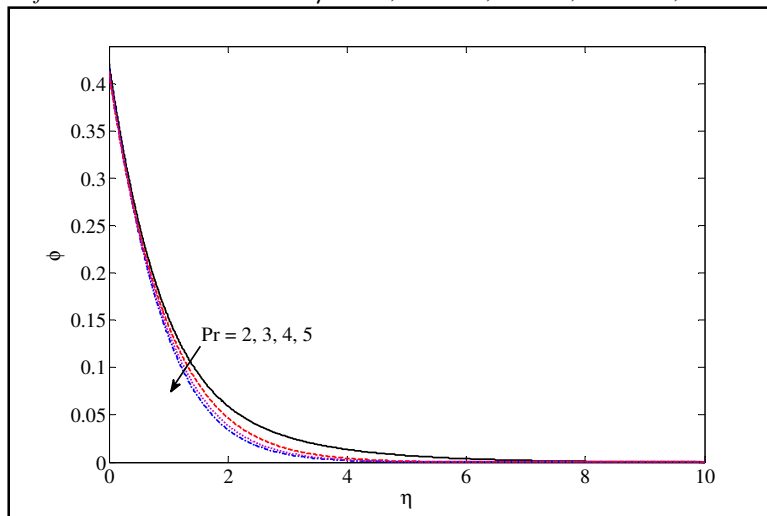


Figure 6(b): Nanoparticle volume fraction profile for various  $Pr$  values with  $\gamma = 0.3, K = 0.4, Le = 2, Nt = 0.1, Nb = 0.1, \delta = 0.3, \beta = 0.3$  and  $Kr = 0.6$

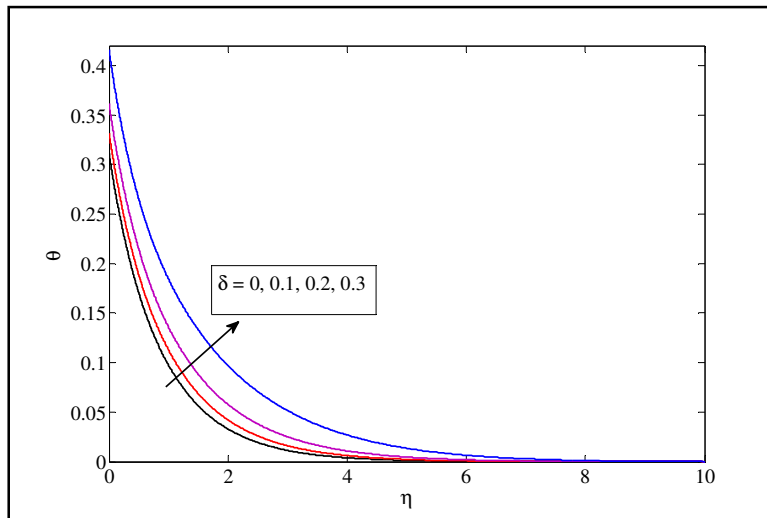


Figure 7: Temperature profile for various  $\delta$  values with  $Pr = 2, K = 0.4, Le = 2, Nt = 0.1, Nb = 0.1, \gamma = 0.3, \beta = 0.3$  and  $Kr = 0.6$

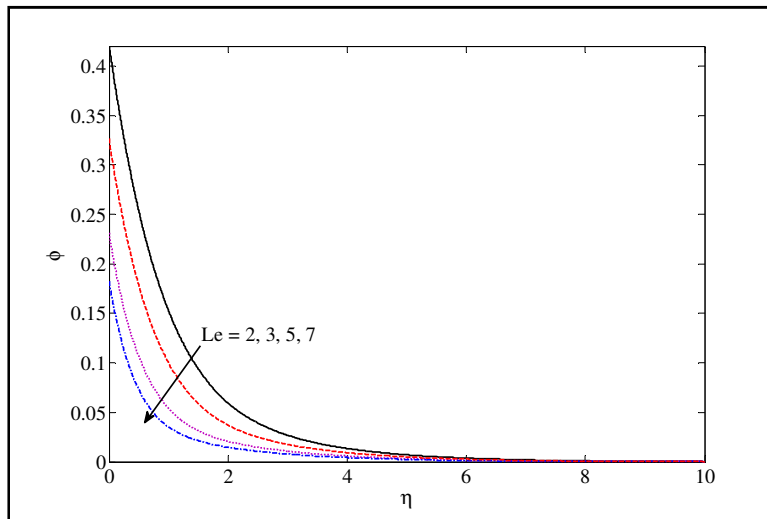


Figure 8: Nanoparticle volume fraction profile for various  $Le$  values with  $Pr = 2, K = 0.4, \gamma = 0.3, Nt = 0.1, Nb = 0.1, \delta = 0.3, \beta = 0.3$  and  $Kr = 0.6$

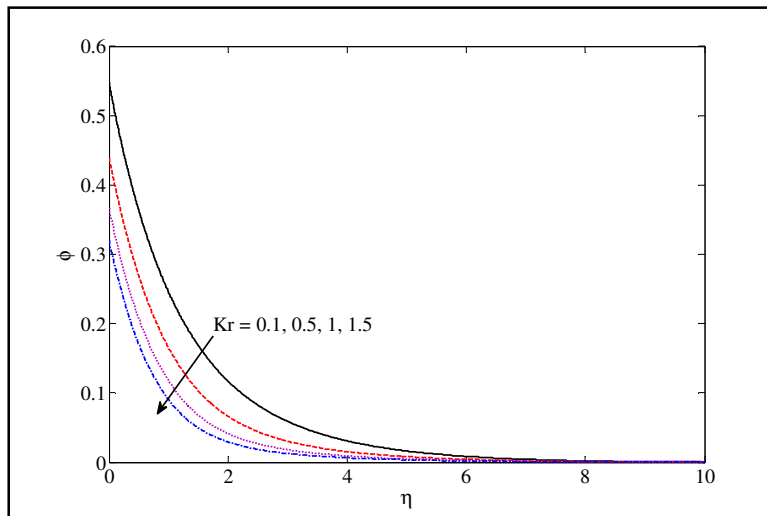


Figure 9: Nanoparticle volume fraction profile for various  $Kr$  values with  $Pr = 2, K = 0.4, Le = 2, Nt = 0.1, Nb = 0.1, \delta = 0.3, \beta = 0.3$  and  $\gamma = 0.3$

$-f''(0)$	Present Study	Magyari and Keller (1999)	Bhattacharyya and Layek (2014)
	1.281809	1.281808	1.28180838

Table 1: Comparison for  $-f''(0)$  for  $K=0$

K	$ f''(0) $
0.1	3.316625
0.2	2.449490
0.3	2.081666
0.4	1.870824

Table 2: Numerical values of magnitude of the skin-friction coefficient  $|f''(0)|$  for various values of  $K$  when  $Nt = 0.1, Nb = 0.1, Kr = 0.1, \delta = 0.1, \gamma = 0.1, Pr = 2$  &  $Le = 2$ .

K	Pr	Nt	Nb	Le	$\delta$	Kr	$\gamma$	$\beta$	$-\theta'(0)$	$-\phi'(0)$
0.1	2	0.1	0.1	2	0.1	0.1	0.1	0.1	0.114263	0.118994
0.2	2	0.1	0.1	2	0.1	0.1	0.1	0.1	0.110483	0.115769
0.3	2	0.1	0.1	2	0.1	0.1	0.1	0.1	0.109408	0.114438
0.4	2	0.1	0.1	2	0.1	0.1	0.1	0.1	0.108886	0.113701
0.4	3	0.1	0.1	2	0.1	0.1	0.1	0.1	0.106466	0.113834
0.4	4	0.1	0.1	2	0.1	0.1	0.1	0.1	0.105280	0.113955
0.4	5	0.1	0.1	2	0.1	0.1	0.1	0.1	0.104552	0.114058
0.4	2	0.2	0.1	2	0.1	0.1	0.1	0.1	0.108924	0.119387
0.4	2	0.4	0.1	2	0.1	0.1	0.1	0.1	0.109003	0.130742
0.4	2	0.6	0.1	2	0.1	0.1	0.1	0.1	0.109083	0.142076
0.4	2	0.1	0.2	2	0.1	0.1	0.1	0.1	0.108915	0.110853
0.4	2	0.1	0.4	2	0.1	0.1	0.1	0.1	0.108974	0.109430
0.4	2	0.1	0.6	2	0.1	0.1	0.1	0.1	0.109034	0.108955
0.4	2	0.1	0.1	3	0.1	0.1	0.1	0.1	0.108881	0.110107
0.4	2	0.1	0.1	4	0.1	0.1	0.1	0.1	0.108877	0.108170
0.4	2	0.1	0.1	5	0.1	0.1	0.1	0.1	0.108875	0.106945
0.4	2	0.1	0.1	2	0.2	0.1	0.1	0.1	0.109502	0.113706
0.4	2	0.1	0.1	2	0.25	0.1	0.1	0.1	0.109934	0.113758
0.4	2	0.1	0.1	2	0.3	0.1	0.1	0.1	0.109501	0.113721
0.4	2	0.1	0.1	2	0.1	0.3	0.1	0.1	0.108885	0.112375
0.4	2	0.1	0.1	2	0.1	0.6	0.1	0.1	0.108883	0.110999
0.4	2	0.1	0.1	2	0.1	1.0	0.1	0.1	0.108881	0.109739
0.4	2	0.1	0.1	2	0.1	0.1	0.2	0.1	0.239233	0.120501
0.4	2	0.1	0.1	2	0.1	0.1	0.3	0.1	0.398641	0.128800
0.4	2	0.1	0.1	2	0.1	0.1	0.4	0.1	0.599138	0.139208
0.4	2	0.1	0.1	2	0.1	0.1	0.1	0.3	0.108966	0.406134
0.4	2	0.1	0.1	2	0.1	0.1	0.1	0.6	0.109169	1.137595
0.4	2	0.1	0.1	2	0.1	0.1	0.1	1.0	0.110035	4.068829

Table 3: Numerical values of  $-\theta'(0), -\phi'(0)$  for various values of  $K, Nt, Nb, Kr, \delta, \gamma, Pr$  and  $Le$ .

6. References

- i. Bhattacharyya Krishnendu and Layek, G. C., (2014), Magnetohydrodynamic Boundary Layer Flow of Nanofluid over an Exponentially Stretching Permeable Sheet, Hindawi Publishing Corporation, Physics Research International Volume 2014, Article ID 592536, 12 pages.
- ii. Buongiorno, J., (2006), Convective transport in nanofluids, Journal of heat transfer, Vol. 128, No.3, pp.240-250.
- iii. Choi SUS, Zhang, ZG, Yu, W., Lockwood, F.E & Gruike, EA, (2001), Anomalously thermal conductivity enhancement in nano tube suspensions, Applied Physics Letters, Vol.79, No.14, pp.2252-2254.
- iv. Choi, S. U. S., (1995) "Enhancing thermal conductivity of fluids with nanoparticles in developments and applications of non-Newtonian flows," ASME, FED-vol. 231/MD-vol. 66, pp. 99-105.
- v. Das, M., Mahato, R., Nandkeolyar, R., (2015), Newtonian heating effect on unsteady hydromagnetic Casson fluid flow past a flat plate with heat and mass transfer, Alexandria Engineering Journal, Vol.54, pp.871-879.

- vi. Fekry M Hady, Fouad S Ibrahim, Sahar M Abdel-Gaied and Mohamed R Eid, (2012), Radiation effect on viscous flow of a nanofluid and heat transfer over a nonlinearly stretching sheet, *Nanoscale Research Letters*, Vol.7:229
- vii. Hussanan, A., Khan, I., Shafie, S., (2013), An exact analysis of heat and mass transfer past a vertical plate with Newtonian heating, *J. Appl. Math.* 2013, Article ID: 434571.
- viii. Hussanan, A., Salleh, M.Z., Tahar, R.M., Khan, I., (2014), Unsteady boundary layer flow and heat transfer of a Casson fluid past an oscillating vertical plate with Newtonian heating, *PloS One*, Vol. 9(10), e108763.
- ix. Iswar Chandra Mandal, Swati Mukhopadhyay, (2013), Heat transfer analysis for fluid flow over an exponentially stretching porous sheet with surface heat flux in porous medium, *Ain Shams Engineering Journal*, Vol. 4, pp.103-110.
- x. Jakkula Anand Rao, Gandamalla Vasumathi, Jakkula Mounica, (2015), Joule Heating and Thermal Radiation Effects on MHD Boundary Layer Flow of a Nanofluid over an Exponentially Stretching Sheet in a Porous Medium, *World Journal of Mechanics*, Vol.5, pp.151-164
- xi. Khan, W. A.and Pop, I., (2010), Boundary-layer flow of a nanofluid past a stretching sheet,*International Journal of Heat and MassTransfer*, Vol. 53, No. 11-12, pp. 2477–2483.
- xii. Magyari, E., and Keller, B., (1999), Heat and mass transfer in the boundary layers on an exponentially stretching continuous surface, *Journal of Physics D*, Vol. 32, No. 5, pp. 577-585.
- xiii. Merkin, J.H., (1994), Natural-convection boundary-layer flow on a vertical surface with Newtonian heating, *Int. J. Heat Fluid Flow*, Vol.15 (5), pp.392–398.
- xiv. Ralston, Wilf, (1960), *Mathematical Methods for Digital Computers*, John Wiley and Sons, N.Y., 117.
- xv. Wang Chaoyang and Tu Chuanjing, (1989), Boundary-layer flow and heat transfer of non-Newtonian fluids in porous media, *Int. d. Heat and Fluid Flow*, Vol. 10, No. 2, June 1989, pp.160-165.
- xvi. RamReddy, Ch., Pradeepa, T. and Srinivasacharya, D., (2015), Similarity Solution for Free Convection Flow of a Micropolar Fluid under Convective Boundary Condition via Lie Scaling Group Transformations, *Hindawi Publishing Corporation, Advances in High Energy Physics*, Vol. 2015, Article ID 650813, 16 pages